B. Metherall C. S. Bohun

March 17, 2020

Abstract

1 Introduction

Tuneable lasers have the ability to vary the frequency of its output by up to about 100 nanometres [1–3] and simultaneously lase at all frequencies within this bandwidth in short pulses. This tuneability leads to applications such as optical coherence tomography [1, 3, 4], coherent anti-Stokes Raman spectroscopy [4], deep tissue multi-photon microscopy [5, 6], and diagnostics of ultrafast processes [4, 7]. Tuneable lasers are usually constructed in a ring with five components: an output coupler, chirped fibre Bragg grating (CFBG), modulator, Er-doped fibre, and a pump laser. A typical tuneable ring laser cavity is depicted in Figure 1. Due to the high power and short duratino of the pulses, the Kerr nonlinearity becomes crucial to the dynamics within the cavity.

The nonlinearity causes several effects to arise within the laser cavity due to the interplay of dispersion, modulation, and the nonlinearity [1, 8–11]. The effect of most interest for this paper is optical wave breaking which causes the leading edge of a pulse to be red shifted, and the trailing edge blue shifted[1] to the point that a shock is developed [12–16]. The shift in frequencies cause the pulse to become rectangular in the frequency domain with a linear chirp over most of the pulse. Wave breaking manifests from self-phase modulation (SPM) which is a direct effect of the nonlinearity causing the pulse to interfere with itself. This interference generates new frequencies which induces the rectangular profile [11, 17, 18]. Modulation instablility is another effect that will be of interest that typically arises in the anomalous dispersion regime. However, in the presence of multiple pulses modulation instability can emerge in the normal dispersion regime as well through cross-phase modulation (XPM) and four-wave mixing (FWM) [17, 19–21]. Modulation instability causes a wave to break into short pulses, and can cause a laser to lose coherence [8, 19, 21]. Within a ring laser cavity wave breaking and modulation instability can become parasitic leading to an unstable and unsustainable pulse. This gives rise to the need of understanding the rich landscape of the parameter space, and determining design principles to guarantee the ring laser is stable and sustainable [1, 9, 11, 22, 23].

*** Paragraph explaining method / results / layout

2 Modelling Efforts

The standard equation for studying nonlinear optics is the nonlinear Schrödinger equation (NLSE),

$$\frac{\partial A}{\partial z} = -i\frac{\beta_2}{2}\frac{\partial^2 A}{\partial T^2} + i\gamma|A|^2 A. \tag{1}$$

Here $A = A(T, z) : \mathbb{R}^2 \mapsto \mathbb{C}$ is the complex pulse amplitude, $\beta_2 \in \mathbb{R}$ is the second order dispersion, and $\gamma \in \mathbb{R}$ is the coefficient of nonlinearity. In practice, the NLSE, (1), lacks a few key terms, thus, it is often generalized by adding amplification and loss[2]. These additions give the generalized nonlinear Schrödinger equation (GNLSE) [1, 17, 23–26],

$$\frac{\partial A}{\partial z} = -i\frac{\beta_2}{2}\frac{\partial^2 A}{\partial T^2} + i\gamma|A|^2 A + \frac{1}{2}g(A)A - \alpha A, \tag{2}$$

where $g(A)$ is an amplifying term due to the gain, and $\alpha \in \mathbb{R}^+$ is the loss due to scattering and absorption.

The GNLSE has many applications in nonlinear optics and fibre optic communications, however, in laser physics typically a modulation term is also added to ensure mode-locking, this yields the master equation of mode-locking [28–34],

$$\frac{\partial A}{\partial z} = -i\frac{\beta_2}{2}\frac{\partial^2 A}{\partial T^2} + i\gamma|A|^2 A + \frac{1}{2}g(A)A - \alpha A - M(T). \tag{3}$$

No analytic solution is known for (3)—even after making the assumptions that the gain is constant, and the modulation is quadratic [28, 29, 35]. However, by neglecting certain terms of (3) analytic solutions can be found [4, 29–31, 33–36]. Furthermore, see Haus [32] for a comprehensive description and history of the theory of mode-locked lasers.

2.1 Discrete Models

Unfortunately, the master equation, (3), is not completely representative of the underlying physics within our laser cavity. In the derivation of (3) it is assumed each process affects the pulse continuously within the cavity. As highlighted by Figure 1, this can be a poor assumption. Within the cavity, each effect is localized to its corresponding component: almost all of the dispersion happens within the

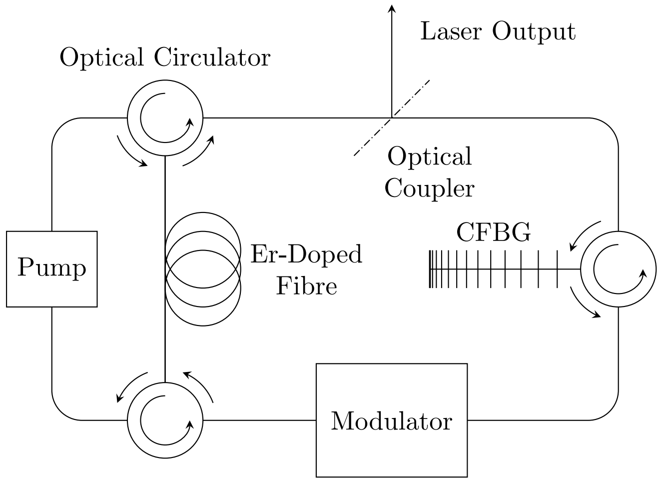

Figure 1: Typical cavity of a fibre ring tuneable laser [4, 5, 9, 10, 27]. The laser pulses travel clockwise around each loop.

[1]In the anomalous dispersion regime, the effect is reversed.

[2]Occasionally higher order terms are added as well.

CFBG [37], the pulse is only amplified within the Erbium-doped fibre, etc. Thus, a better model is one where we consider a simplified version of the master equation, (3), for each component. Solving these simplified differential equations yields an algebraic expression for the effect of each individual component. The relations can then be functionally composed to give an iterative map for the effect of one round trip of the cavity.

Such a method was first proposed in 1955 by Cutler [38] while analyzing a microwave regenerative pulse generator. This method was adapted for mode-locked lasers in 1969 by Siegman and Kuizenga [39–42]. The effects of the nonlinearity would not be considered until Martinez, Fork, and Gordon [43,44] tried modelling passively mode-locked lasers. This issue has recently been readdressed by Burgoyne [4] in the literature for tuneable lasers. In each of these models the effect of each block is described by a transfer function.

Despite the development of these block style models, several short-comings exist. The clearest is that none of these models have contained every block—either the nonlinearity or the modulation have been omitted. Each component of a tuneable plays a crucial role and the laser will not function correctly without the inclusion of all of the components. Another drawback is that the functional operations of some of the components used in their models are phenomenological. While these functions are chosen based on the observed output, they are not necessarily consistent with the underlying physics. Finally, none of these previous models have been able to fully exhibit the instabilities described in Section 1.

3 Model Derivation

Using the idea of a discrete model presented Section 2.1, we derive our model from the GNLSE, (2); however, in the case of the modulation we consider the exact functional form to be determined by the laser operator. To accomplish this we follow the method described in Section 2.1; we neglect all terms but one on the right side of (2) and solve the simplified differential equations.

To proceed we must choose the form of the amplification term, $g(A)$. We assume the gain has the form

$$g(A) = \frac{g_0}{1 + E/E_{\text{sat}}}, \qquad E = \int_{-\infty}^{\infty} |A|^2 \, \mathrm{d}T, \tag{4}$$

where g_0 is a small signal gain, E is the energy of the pulse, and E_{sat} is the energy at which the gain begins to saturate [7, 25, 28]. This reduces the GNLSE, (2), to

$$\frac{\partial A}{\partial z} = \frac{g_0 A}{2(1 + E/E_{\text{sat}})}. \tag{5}$$

By assuming $E(0) = E$ and $E(L_g) = E_{\text{out}}$, we find the energy after amplification is

$$E_{\text{out}} = E_{\text{sat}} W\left(\frac{E}{E_{\text{sat}}} \mathrm{e}^{E/E_{\text{sat}}} \mathrm{e}^{g_9 L_g}\right), \tag{6}$$

where W is the Lambert W function [45]. Rewriting (6) in terms of the pulse gives

$$G(A) = \left(\frac{E_{\text{sat}}}{E} W\left(\frac{E}{E_{\text{sat}}} \mathrm{e}^{E/E_{\text{sat}}} \mathrm{e}^{g_0 L_g}\right)\right)^{1/2} A \tag{7}$$

for the amplification of the pulse within the Er-doped fibre. Repeating this process for the loss, dispersion, and nonlinearity yields

$$L(A) = (1 - R)\mathrm{e}^{-\alpha L_T} A, \tag{8}$$

$$D(A) = \mathcal{F}^{-1}\Big\{\mathrm{e}^{i\omega^2 L_D \beta_2/2} \mathcal{F}\{A\}\Big\}, \tag{9}$$

$$F(A) = A\mathrm{e}^{i\gamma |A|^2 L_f}, \tag{10}$$

where R is the reflectivity of the output coupler[3], L_T is the total length of the laser circuit, L_D is the length of the dispersive medium, L_f is the length of fibre between the amplifier and the output coupler, and where $\mathcal{F}$ denotes the Fourier transform. Finally, we must assume a form for the modulation. The modulation is considered to be applied externally in which ever way the operator sees fit. For simplicity the representation is taken as the Gaussian

$$M(A) = \mathrm{e}^{-T^2/2T_M^2} A, \tag{11}$$

where T_M is the characteristic width of the modulation. This assumption is not particularly restrictive. Calcaterra and Boldt have shown that Gaussians can form a basis for $L^2(\mathbb{R})$ [46]. Therefore, we can approximate any modulation function in $L^2(\mathbb{R})$ by a sum of (11).

3.1 Non-Dimensionalization

The structure of each process of the laser can be better understood by re-scaling the time, energy, and amplitude; this suggests the convenient scalings:

$$T = T_M \widetilde{T}, \qquad E = E_{\text{sat}} \widetilde{E}, \qquad A = \left(\frac{E_{\text{sat}}}{T_M}\right)^{1/2} \widetilde{A}. \tag{12}$$

Revisiting each process map shows each process has a characteristic non-dimensional parameter. The new mappings—after dropping the tildes—are

$$\begin{aligned} &G(A) = \big(E^{-1} W\big(aE\mathrm{e}^{E}\big)\big)^{1/2} A, \quad F(A) = A\mathrm{e}^{ib|A|^2}, \\ &D(A) = \mathcal{F}^{-1}\Big\{\mathrm{e}^{is^2\omega^2} \mathcal{F}\{A\}\Big\}, \qquad L(A) = hA, \\ &M(A) = \mathrm{e}^{-T^2/2} A, \end{aligned} \tag{13}$$

with the four dimensionless parameters,

$$\begin{aligned} &a = \mathrm{e}^{g_0 L_g} \sim 8 \times 10^3, \qquad &&h = (1 - R)\mathrm{e}^{-\alpha L} \sim 0.04, \\ &b = \gamma L_f \frac{E_{\text{sat}}}{T_M} \sim 1, &&s = \sqrt{\frac{\beta_2 L_D}{2T_M^2}} \sim 0.2, \end{aligned} \tag{14}$$

which characterize the behaviour of the laser. Nominal values for the parameters, (14), can be found in [1, 3, 4, 15, 17, 22–26, 33, 34, 37, 47–49]. Notice that the modulation is only characterized by T_M, and each other process has its own associated independent non-dimensional parameter.

3.2 Combining the Effects

Now that we have the algebraic effect of each section of the cavity, we are ready to compose each map together to give the effect of one round trip of the cavity. Thus, we must now consider the order of the components. As we are most interested in the output of the laser cavity, we shall start with the

[3] Depending on the layout of the laser cavity the loss may instead take the form $L(A) = R\mathrm{e}^{-\alpha L_T} A$.

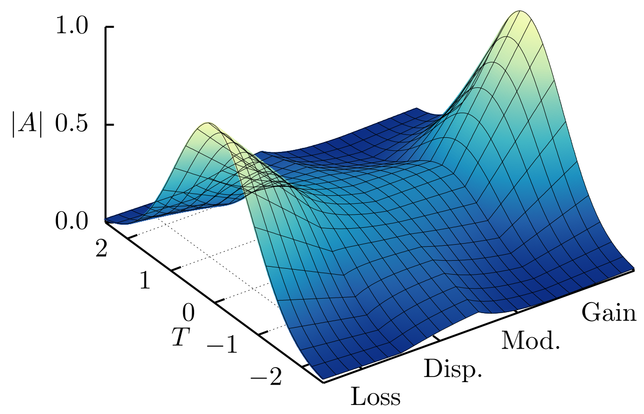

Figure 2: Evolution of the envelope during one round trip of the cavity at equilibrium. The pulse decays due to the output coupler, dispersed by the CFBG, modulated by the modulator, and finally amplified by the gain fibre (the envelope is unaltered by the nonlinearity). Note that this is for visualization only, the durations are not to scale.

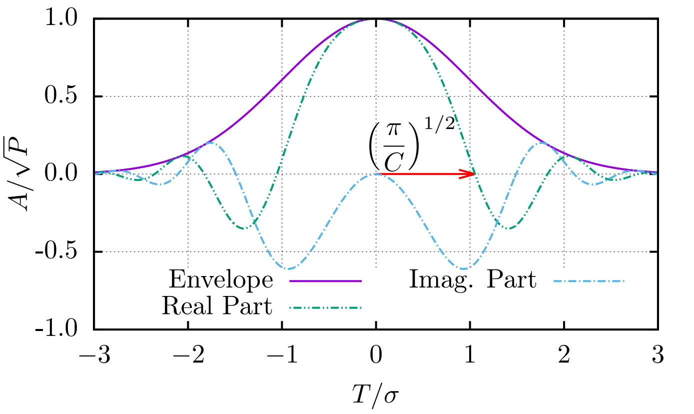

Figure 3: Solution to the linear model given by (16).

loss. We then pass the pulse through the CFBG followed by the modulator. The pulse then travels through the Er-doped fibre to be amplified, and finally we consider the effect of the nonlinearity. The nonlinearity must immediately follow the gain—this is the section of the cavity where the pulse is most energetic, and hence, has the largest effect. Note, the permutation of the other components is indeed important as the operators do not, in general, commute—this is in contrast to the models described in Section 2.1. Moreover, we prefer the loss to follow the gain and nonlinearity as we wish to minimize the length over which the nonlinearity has an effect, and maximize the output power. Functionally we denote one round trip of the cavity by

$$\mathcal{L}(A) = F(G(M(D(L(A))))). \tag{15}$$

The pulse after one complete circuit of the laser cavity is then returned back into the cavity to restart the process. A steady solution to this model is one in which the envelope and chirp are unchanged after traversing every component in the cavity—we are uninterested in the phase. That is, such that $\mathcal{L}(A) = A\mathrm{e}^{i\phi}$—for some $\phi \in \mathbb{R}$. An example of the evolution of the envelope during one round trip of the laser cavity can be found in Figure 2.

4 Results

We split the results into two subsections. In the following subsection we investigate the low nonlinearity limit, and in Section 4.2 we look at the full nonlinear model.

4.1 Linear Solution

By neglecting the effect of the nonlinearity, that is, $b = 0$, a solution can be found analytically. We assume the solution will take the form of a chirped Gaussian. There are a few reasons for this; the solution to the models presented in [38,39,42–44] were Gaussian, the equilibrium shape will be highly correlated to the shape of the modulation function, and since a Gaussian is a fixed point of the Fourier transform [50]. Furthermore, this form is chosen because it resembles the envelope and linear chirp expected [4,29,32,34,35].

To compute $\mathcal{L}(A)$, consider the pulse

$$A = \sqrt{P}\exp\left(-(1+iC)\frac{T^2}{2\sigma^2}\right)\mathrm{e}^{i\phi_0}, \tag{16}$$

where P is the peak power, C is the chirp, σ^2 is the variance, and ϕ_0 is the initial phase. This pulse shape is depicted in Figure 3.

To compute $\mathcal{F}(A)$, given the initial pulse (16), we iteratively compute the effect of each process map from (13). Now, by equating $\mathcal{F}(A)$ and $A\mathrm{e}^{i\phi}$ we obtain a system of equations. In particular,

$$\sigma^8 + 4s^4\sigma^6 - 20s^4\sigma^4 + 32s^4\sigma^2 - 16s^4 = 0, \tag{17}$$

$$C = \frac{\sigma^4 \pm \sqrt{\sigma^8 - 16s^4(1-\sigma^2)^2}}{4s^2(1-\sigma^2)}. \tag{18}$$

As (17) is a quartic in σ^2 it has an analytic solution, namely,

$$\sigma^2 = \sqrt{2}s\left(s^6 + 3s^2 + \sqrt{4+s^4}(1+s^4)\right)^{1/2} - s^4 - s^2\sqrt{4+s^4}, \tag{19}$$

which can readily be used to find the chirp, C. By asymptotically expanding (17) we find the useful relations

$$\sigma^2 \sim \begin{cases} 2s(1-s) + \mathcal{O}(s^3) & s \to 0 \\ 1 - \frac{1}{4}s^{-4} + \frac{3}{8}s^{-8} + \mathcal{O}(s^{-12}) & s \to \infty, \end{cases} \tag{20}$$

$$C \sim \begin{cases} 1 - s + \frac{1}{2}s^2 + \mathcal{O}(s^3) & s \to 0 \\ \frac{1}{2}s^{-2} - \frac{3}{8}s^{-6} + \mathcal{O}(s^{-10}) & s \to \infty. \end{cases} \tag{21}$$

The equilibrium energy and peak power can be found by conservation of energy to give

$$E = \frac{h^2(1-\sigma^2)^{1/2}}{1 - h^2(1-\sigma^2)^{1/2}}\log\left(ah^2(1-\sigma^2)^{1/2}\right), \tag{22}$$

and

$$P = \frac{W(aE\mathrm{e}^E)}{\sqrt{\pi}\sigma}, \tag{23}$$

respectively.

Our linearized model indeed exhibits the same form as previous linear models. However, by including the effects of the nonlinearity we uncover the rich interplay between dispersion, modulation, and nonlinearity not previously found mathematically.

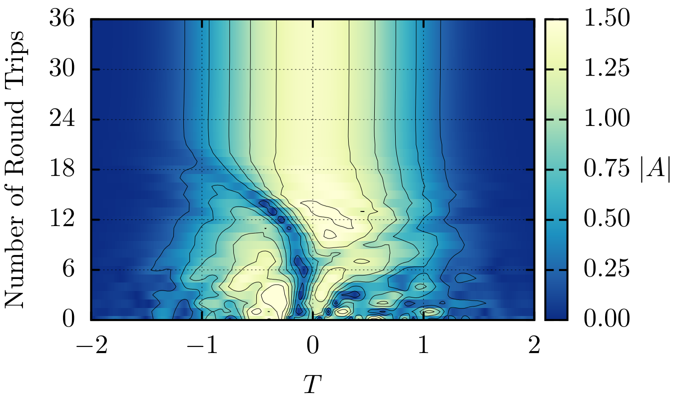

(a) Example of a pulse stabilizing from a seemingly random initial pulse shape ($b = 1.0$).

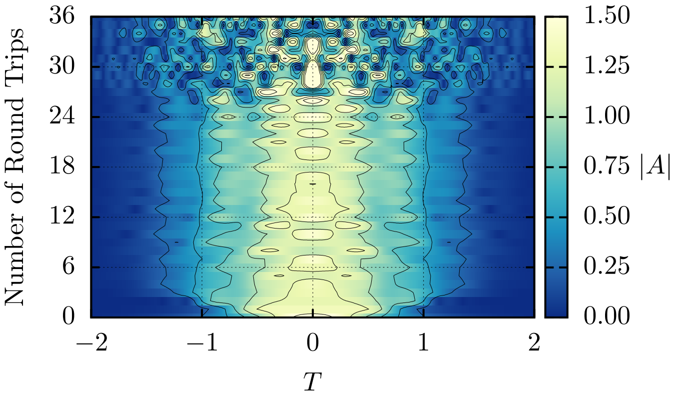

(b) Example of a pulse destabilizing from a hyperbolic secant initial pulse ($b = 1.6$).

Figure 4: Two extremes of the evolution of a pulse ($s = 0.1$, $E_0 = 0.1$, $a = 8000$, $h = 0.04$).

4.2 Nonlinear Solution and Instability

In this iterative scheme—as well as within the laboratory—we must specify the input pulse shape. The most common form is a hyperbolic secant [8,14,15,23,51], which we assume has the exact form

$$A_0 = \Gamma \operatorname{sech}(2T) e^{i\pi/4}, \tag{24}$$

where Γ is a normalizing factor chosen so the pulse has an initial energy of $E_0 = 0.1$, unless specified otherwise. We plot the evolution of a pulse through the cavity in Figure 4. We find very different behaviour in these two examples despite very similar parameters. In Figure 4a the input pulse is very noisy, but, sheds off the left lobe and reaches an equilibrium state quickly after. In the opposite extreme, Figure 4b has the smooth initial pulse given in (24), however, the nonlinearity causes the pulse to pulsate or 'breathe'. This effect compounds with each round trip, which ultimately results in the degradation of the pulse into an unusable and unrecoverable state. The only difference between these two realizations, besides the initial pulse shape, is the value of the nonlinearity parameter, b.

stability
instability
energy
error
permutation
chirp / chirp Saturation
shape / kurtosis

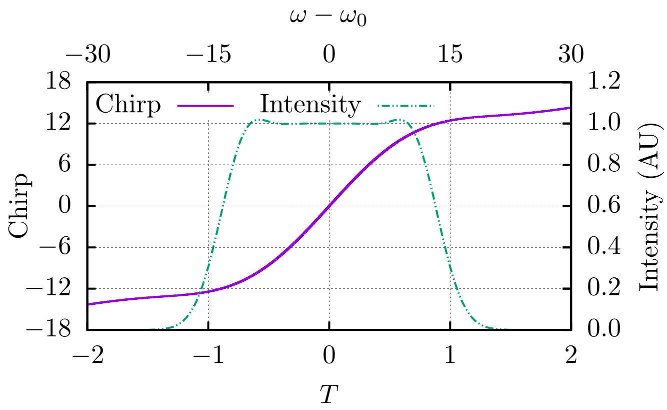

Figure 5

In the nonlinear case, we recover this linear response for moderate values of T. However, for $|T| > 1$ the chirp begins to saturate. This is consistent with the experimental results [?, ?, ?].

Wave breaking is not limited to just optics; wave breaking occurs in areas such as plasmas, transmission lines, and fluid dynamics [?]. Wave breaking occurs because the pulse begins to interfere with itself in a way called SPM [?,17,37]. SPM occurs because the index of refraction is intensity dependent [?, ?, ?, 37], which leads to additional chirp across the pulse [?, ?, ?, 17]. This in turn causes higher order frequencies to be injected into the pulse [?, 17],

We obtain comparable results as in the experiments [?, ?]

To obtain a better understanding of how the pulse either converges to equilibrium, or diverges to wave breaking, we shall examine the difference between the envelopes of consecutive iterations. More precisely, we compute the error by

$$\mathrm{E} = \frac{\| |A_i| - |A_{i-1}| \|_2}{\|A_{i-1}\|_2}, \tag{25}$$

where $\| \cdot \|_2$ denotes the $L^2(\mathbb{R})$ norm, which is computed numerically using the trapezoid rule ($N = 2^{18}$).

he standard method would be to iterate until a fixed tolerance is reached, however, there are some reasons that make a fixed number of iterations preferable—as long as a sufficient number is chosen. The main reason is that this allows us to observe a richer structure than simply whether or not the tolerance had been reached by some maximum number of iterations. Additionally, incorrectly choosing the critical tolerance could easily lead to erroneous categorizations at points.

The last item we wish to consider is the order in which the components are placed.

xpm [17, 19, 20]

5 Conclusion

References

[1] C. S. Bohun, Y. Cher, L. J. Cummings, P. Howell, T. Mitre, L. Monasse, J. Mueller, and S. Rouillon, "Modelling and Specifying Dispersive Laser Cavities," in *Sixth Montréal Industrial Problem Solving Workshop*, pp. 11–25, 2015.

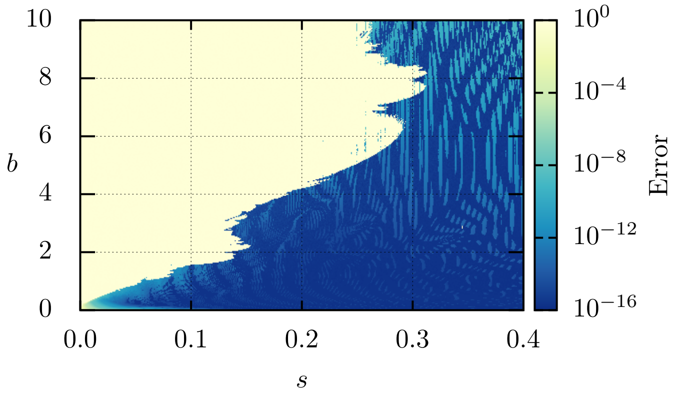

Figure 6

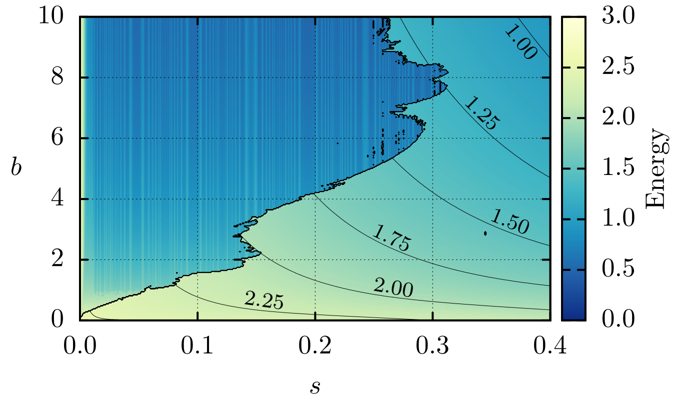

Figure 7

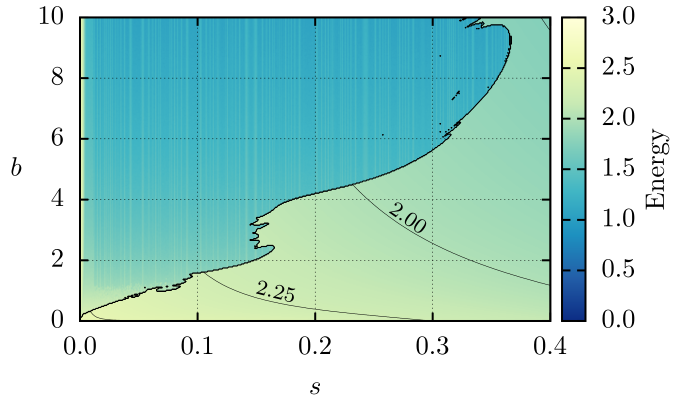

Figure 8

[2] B. Burgoyne and A. Villeneuve, "Programmable Lasers: Design and Applications," in *Proc.SPIE*, vol. 7580, 2010.

[3] S. Yamashita, Y. Nakazaki, R. Konishi, and O. Kusakari, "Wide and Fast Wavelength-Swept Fiber Laser Based on Dispersion Tuning for Dynamic Sensing," *Journal of Sensors*, vol. 2009, 2009.

[4] B. Burgoyne, A. Dupuis, and A. Villeneuve, "An Experimentally Validated Discrete Model for Dispersion-Tuned Actively Mode-Locked Lasers," *IEEE Journal of Selected Topics in Quantum Electronics*, vol. 20, pp. 390–398, Sept 2014.

[5] H. Chung, W. Liu, Q. Cao, F. X. Kärtner, and G. Chang, "Er-Fiber Laser Enabled, Energy Scalable Femtosecond Source Tunable from 1.3 to 1.7 μm," *Opt. Express*, vol. 25, pp. 15760–15771, Jul 2017.

[6] W. Liu, S. Chia, H. Chung, R. Greinert, F. X. Kärtner, and G. Chang, "Energetic Ultrafast Fiber Laser Sources Tunable in 1030–1215 nm for Deep Tissue Multi-Photon Microscopy," *Opt. Express*, vol. 25, pp. 6822–6831, Mar 2017.

[7] W. T. Silfvast, *Laser Fundamentals*. Cambridge University Press, 2 ed., 2004.

[8] S. Coen and M. Haelterman, "Modulational Instability Induced by Cavity Boundary Conditions in a Normally Dispersive Optical Fiber," *Phys. Rev. Lett.*, vol. 79, pp. 4139–4142, Nov 1997.

[9] C. Lapre, C. Billet, F. Meng, P. Ryczkowski, T. Sylvestre, C. Finot, G. Genty, and J. M. Dudley, "Real-Time Characterization of Spectral Instabilities in a Mode-Locked Fibre Laser Exhibiting Soliton-Similariton Dynamics," *Sci Rep*, vol. 9, Sept 2019.

[10] G. D. Shao, X. Hu, J. Guo, Y. F. Song, L. M. Zhao, D. Y. Shen, and D. Y. Tang, "Cavity-Assisted Modulation Instability Lasing of a Fiber Ring Laser," *Applied Physics B*, vol. 125, no. 5, 2019.

[11] R. I. Woodward, "Dispersion Engineering of Mode-Locked Fibre Lasers," *Journal of Optics*, vol. 20, p. 033002, Feb 2018.

[12] D. Anderson, M. Desaix, M. Lisak, and M. L. Quiroga-Teixeiro, "Wave Breaking in Nonlinear-Optical Fibers," *J. Opt. Soc. Am. B*, vol. 9, pp. 1358–1361, Aug 1992.

[13] J. E. Rothenberg and D. Grischkowsky, "Observation of the Formation of an Optical Intensity Shock and Wave Breaking in the Nonlinear Propagation of Pulses in Optical Fibers," *Phys. Rev. Lett.*, vol. 62, pp. 531–534, Jan 1989.

[14] J. E. Rothenberg, "Femtosecond Optical Shocks and Wave Breaking in Fiber Propagation," *J. Opt. Soc. Am. B*, vol. 6, pp. 2392–2401, Dec 1989.

[15] W. J. Tomlinson, R. H. Stolen, and C. V. Shank, "Compression of Optical Pulses Chirped by Self-Phase Modulation in Fibers," in *Conference on Lasers and Electro-Optics*, pp. 139–149, Optical Society of America, 1984.

[16] W. J. Tomlinson, R. H. Stolen, and A. M. Johnson, "Optical Wave Breaking of Pulses in Nonlinear Optical Fibers," *Opt. Lett.*, vol. 10, pp. 457–459, Sept 1985.

[17] G. Agrawal, *Nonlinear Fiber Optics.* Academic Press, 5 ed., 2013.

[18] L. F. Mollenauer, R. H. Stolen, and J. P. Gordon, "Experimental Observation of Picosecond Pulse Narrowing and Solitons in Optical Fibers," *Phys. Rev. Lett.*, vol. 45, pp. 1095–1098, Sep 1980.

[19] G. P. Agrawal, "Modulation Instability Induced by Cross-Phase Modulation," *Phys. Rev. Lett.*, vol. 59, pp. 880–883, Aug 1987.

[20] G. P. Agrawal, P. L. Baldeck, and R. R. Alfano, "Temporal and Spectral Effects of Cross-Phase Modulation on Copropagating Ultrashort Pulses in Optical Fibers," *Phys. Rev. A*, vol. 40, pp. 5063–5072, Nov 1989.

[21] M. Haelterman, S. Trillo, and S. Wabnitz, "Additive-Modulation-Instability Ring Laser in the Normal Dispersion Regime of a Fiber," *Opt. Lett.*, vol. 17, pp. 745–747, May 1992.

[22] B. Burgoyne. Private Communication, 2018.

[23] C. Finot, B. Kibler, L. Provost, and S. Wabnitz, "Beneficial Impact of Wave-Breaking for Coherent Continuum Formation in Normally Dispersive Nonlinear Fibers," *J. Opt. Soc. Am. B*, vol. 25, pp. 1938–1948, Nov 2008.

[24] J. Peng, H. Luo, and L. Zhan, "In-Cavity Soliton Self-Frequency Shift Ultrafast Fiber Lasers," *Opt. Lett.*, vol. 43, pp. 5913–5916, Dec 2018.

[25] O. V. Shtyrina, A. V. Ivanenko, I. A. Yarutkina, A. V. Kemmer, A. S. Skidin, S. M. Kobtsev, and M. P. Fedoruk, "Experimental Measurement and Analytical Estimation of the Signal Gain in an Er-Doped Fiber," *J. Opt. Soc. Am. B*, vol. 34, pp. 227–231, Feb 2017.

[26] I. Yarutkina, O. Shtyrina, M. Fedoruk, and S. Turitsyn, "Numerical Modeling of Fiber Lasers with Long and Ultra-long Ring Cavity," *Opt. Express*, vol. 21, pp. 12942–12950, May 2013.

[27] D. Tang, J. Guo, Y. Song, L. Li, L. Zhao, and D. Shen, "GHz Pulse Train Generation in Fiber Lasers by Cavity Induced Modulation Instability," *Optical Fiber Technology*, vol. 20, no. 6, pp. 610–614, 2014. Short Pulse Fiber Lasers.

[28] H. A. Haus, *Waves and Fields in Optoelectronics.* Prentice-Hall, Inc., 1984.

[29] H. A. Haus, "A Theory of Forced Mode Locking," *IEEE Journal of Quantum Electronics*, vol. 11, pp. 323–330, July 1975.

[30] H. A. Haus, "Laser Mode Locking with Addition of Nonlinear Index," *IEEE Journal of Quantum Electronics*, vol. 22, pp. 325–331, Feb 1986.

[31] H. A. Haus, "Analytic Theory of Additive Pulse and Kerr Lens Mode Locking," *IEEE Journal of Quantum Electronics*, vol. 28, pp. 2086–2096, Oct 1992.

[32] H. A. Haus, "Mode-Locking of Lasers," *IEEE Journal of Selected Topics in Quantum Electronics*, vol. 6, pp. 1173–1185, Nov 2000.

[33] K. Tamura and M. Nakazawa, "Dispersion-Tuned Harmonically Mode-Locked Fiber Ring Laser for Self-Synchronization to an External Clock," *Opt. Lett.*, vol. 21, pp. 1984–1986, Dec 1996.

[34] N. G. Usechak and G. P. Agrawal, "Rate-Equation Approach for Frequency-Modulation Mode Locking using the Moment Method," *J. Opt. Soc. Am. B*, vol. 22, pp. 2570–2580, Dec 2005.

[35] H. A. Haus, "Theory of Soliton Stability in Asynchronous Modelocking," *Journal of Lightwave Technology*, vol. 14, pp. 622–627, April 1996.

[36] H. A. Haus, J. G. Fujimoto, and E. P. Ippen, "Structures for Additive Pulse Mode Locking," *J. Opt. Soc. Am. B*, vol. 8, pp. 2068–2076, Oct 1991.

[37] G. Agrawal, *Fiber-Optic Communication Systems.* John Wiley & Sons, Inc., 3 ed., 2002.

[38] C. C. Cutler, "The Regenerative Pulse Generator," in *Proceedings of the IRE*, IEEE, Feb 1955.

[39] D. J. Kuizenga and A. E. Siegman, "FM and AM Mode Locking of the Homogeneous Laser - Part I: Theory," *IEEE Journal of Quantum Electronics*, vol. 6, pp. 694–708, Nov 1970.

[40] D. J. Kuizenga and A. E. Siegman, "FM and AM Mode Locking of the Homogeneous Laser - Part II: Experimental Results in a Nd:YAG Laser with Internal FM Modulation," *IEEE Journal of Quantum Electronics*, vol. 6, pp. 709–715, Nov 1970.

[41] D. J. Kuizenga and A. E. Siegman, "FM-Laser Operation of the Nd:YAG Laser," *IEEE Journal of Quantum Electronics*, vol. 6, pp. 673–677, Nov 1970.

[42] A. E. Siegman and D. J. Kuizenga, "Simple Analytic Expressions for AM and FM Modelocked Pulses in Homogenous Lasers," *Appl. Phys. Lett.*, pp. 181–182, Mar 1969.

[43] O. E. Martinez, R. L. Fork, and J. P. Gordon, "Theory of Passively Mode-Locked Lasers Including Self-Phase Modulation and Group-Velocity Dispersion," *Opt. Lett.*, vol. 9, pp. 156–158, May 1984.

[44] O. E. Martinez, R. L. Fork, and J. P. Gordon, "Theory of Passively Mode-Locked Lasers for the Case of a Nonlinear Complex-Propagation Coefficient," *J. Opt. Soc. Am. B*, vol. 2, pp. 753–760, May 1985.

[45] R. M. Corless, G. H. Gonnet, D. E. G. Hare, D. J. Jeffrey, and D. E. Knuth, "On the Lambert W function," *Advances in Computational Mathematics*, vol. 5, Dec 1996.

[46] C. Calcaterra and A. Boldt, "Approximating with Gaussians," *ArXiv*, May 2008. arXiv:0805.3795.

[47] S. Li and K. T. Chan, "Electrical Wavelength Tunable and Multiwavelength Actively Mode-Locked Fiber Ring Laser," *Applied Physics Letters*, vol. 72, no. 16, pp. 1954–1956, 1998.

[48] N. M. Litchinitser, B. J. Eggleton, and D. B. Patterson, "Fiber Bragg Gratings for Dispersion Compensation in Transmission: Theoretical Model and Design Criteria for Nearly Ideal Pulse Recompression," *Journal of Lightwave Technology*, vol. 15, pp. 1303–1313, Aug 1997.

[49] K. Tamura, E. P. Ippen, H. A. Haus, and L. E. Nelson, "77-fs Pulse Generation from a Stretched-Pulse Mode-Locked All-Fiber Ring Laser," *Opt. Lett.*, vol. 18, pp. 1080–1082, Jul 1993.

[50] I. S. Gradshteyn and I. M. Ryzhik, *Table of Integrals, Series, and Products.* Academic Press, 7 ed., 2007.

[51] F. M. Mitschke and L. F. Mollenauer, "Discovery of the Soliton Self-Frequency Shift," *Opt. Lett.*, vol. 11, pp. 659–661, Oct 1986.